J|A|C|S
COMMUNICATIONS

Published on Web 06/22/2006

Kinetic Analysis for Formation of $Cd_{1-x}Zn_xSe$ Solid-Solution Nanocrystals

Yun-Mo Sung,* Yong-Ji Lee, and Kyung-Soo Park

Department of Materials Science & Engineering, Korea University, Seoul, Korea 136-713

Received March 25, 2006; E-mail: ymsung@korea.ac.kr

CdSe semiconductor colloidal nanocrystals have attracted great attention due to their unique photoabsorption and emission characteristics.[1−5] They show specific quantum confinement effects and thus reveal visible range light emission depending upon each particle size. To improve quantum efficiency, CdSe nanocrystal core is often passivated by another semiconductor shell with a high-energy band gap, such as ZnS, ZnSe, and CdS.[6−8] On the other hand, Han and Knoll[9−11] prepared solid-solution nanocrystals, such as $Cd_{1-x}Zn_xSe$ and $Cd_{1-x}Zn_xS$, by heat treatment of CdSe/ZnSe and CdS/ZnS core/shell nanocrystals, respectively. Their results reveal that solid-solution nanocrystals possess color-tunable light emission depending upon their chemical compositions and narrow light emission spectral width of 14 nm, which is comparable to the homogeneous line width of single CdSe nanocrystals. However, sometimes solid-solution treatment of two semiconductors with different constituent atoms is incomplete, and thus the solid-solution effect on light emission is not predictable. Also, the formation mechanism of $Cd_{1-x}Zn_xSe$ and $Cd_{1-x}Zn_xS$ solid-solutions via heat treatment of core/shell nanocrystals is still unknown. In this study, for the first time, a kinetic equation for the solid-solution formation was established in core/shell nanocrystals as a function of temperature and time, and the solid-solution formation mechanism was elucidated based upon the activation energy.

Most details of the synthesizing methods for CdSe/ZnSe core/shell nanocrystals were similar to those reported in the literatures.[8] Inductively coupled plasma (ICP) analysis on the CdSe/ZnSe nanocrystals revealed the atomic ratio of Cd:Zn:Se was 55:45:100. The synthesized CdSe/ZnSe nanocrystals in chloroform were isothermally heated for the solid-solution treatments at 315, 330, 345, and 360 °C, respectively, for different time periods. The lattice parameter of the *a*-axis (4.153 Å) in $Cd_{0.55}Zn_{0.45}Se$, estimated from the Vegard's law, was used as a measure of complete solid-solution formation.

Figure 1 shows the XRD patterns of CdSe/ZnSe nanocrystals heat treated at different temperatures for different time periods. JCPDS data of CdSe and ZnSe in the Wurtzite structure were indicated at the top and bottom axes as references for comparison. In this kinetic analysis, two important assumptions were employed. First, the ZnSe shell is presumed to be XRD invisible, not giving any change in the CdSe diffraction peaks due to its very small crystallite size. Second, the CdSe core is completely crystalline as prepared, and thus all CdSe in a core can be detected by XRD. Thus, the possibility of the crystallinity increase occurring during the solid-solution heat treatment was excluded. Both of the assumptions were certainly supported by XRD and high-resolution transmission electron microscopy (HRTEM) analyses, respectively.

With an increase of heat treatment time, the XRD peak positions from CdSe core crystals showed apparent shifts to high 2θ angles, indicating the lattice parameter decrease due to the progression of solid-solution formation of $Cd_{1-x}Zn_xSe$. The lattice parameter variation was monitored with heat treatment time period and temperature (see Supporting Information for details). The samples

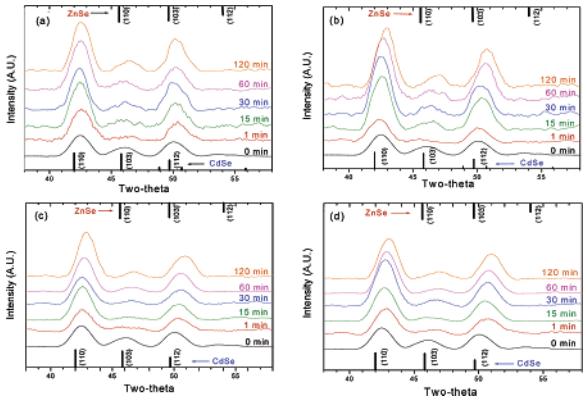

Figure 1. X-ray diffraction (XRD) patterns of CdSe/ZnSe nanocrystals heat treated at (a) 315, (b) 330, (c) 345, and (d) 360 °C for 1, 15, 30, 60, and 120 min, respectively.

heat treated at a high temperature showed rapid decrease in the lattice parameter possibly due to the high mobility of diffusing ions. The degree of solid-solution formation (x) was determined using the Vegard's law, and its variation was also monitored with heat treatment time period and temperature (see Supporting Information for details). The samples heat treated at high temperatures showed a higher rate of solid-solution formation compared to those heat treated at low temperatures, and the result revealed typical sigmoidal variation curves, indicating that a parabolic kinetics is governing the solid-solution formation reactions. The degree of solid-solution formation (x) was used in the Jander analysis[12] to analyze the solid-solution formation mechanism in the CdSe/ZnSe system.

Jander analysis, based upon a parabolic kinetics, has been widely used for the kinetic analysis of chemical reactions occurring in spherical-shaped particles and employed for this study as the following:

$$[1 - (1 - x)^{1/3}]^2 = kt \qquad (1)$$

Here, x is the degree of solid-solution formation, k is the reaction rate constant, and t is the heat treatment time. The Jander plots in Figure 1a showed high linearity until 12 min heat treatment. The reason that the y-intercept values are not approaching exactly zero, especially for 360 °C, is that the solid-solution formation has already progressed during heating the CdSe/ZnSe nanocrystals in chloroform from room temperature up to the corresponding heat treatment temperatures. Thus, the kinetics data even at 1 min can be considered as those at the early stage of solid-solution formation reaction. From the slopes of each linear curve, k values were determined with temperature, and the k values following Arrhenius-type analysis were applied to obtain activation energy for the $Cd_{1-x}Zn_xSe$ solid-solution formation:

$$\ln k = \ln k_o - \frac{Q}{RT} \qquad (2)$$

10.1021/ja061858c CCC: $33.50

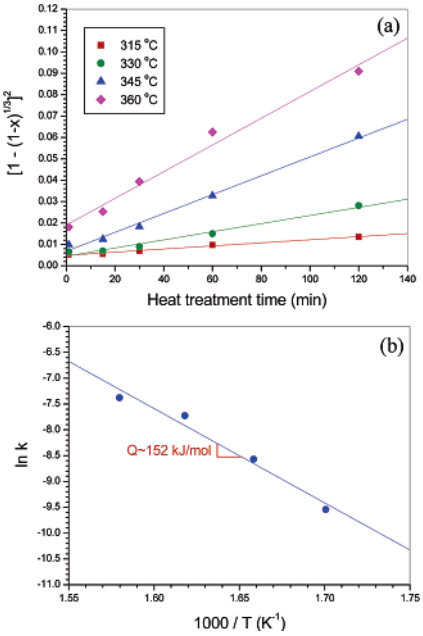

Figure 2. Jander plots of solid-solution formation reaction in CdSe/ZnSe nanocrystals (a) and Arrhenius plot of solid-solution formation reaction in CdSe/ZnSe nanocrystals (b).

Here, k_o is a constant, R is the gas constant in J/mol·K, Q is the activation energy for solid-solution formation, and T is the heat treatment temperature. From the slope of the Arrhenius plot shown in Figure 2b, the activation energy for the solid-solution formation was determined as ~152 kJ/mol. This activation energy value is slightly higher than the bond strength of $Zn^{2+}-Se^{2-}$, 136 kJ/mol, and much lower than that of $Cd^{2+}-Se^{2-}$, 310 kJ/mol. Thus, it can be concluded that the mechanism of $Cd_{1-x}Zn_xSe$ solid-solution formation via heat treatment of CdSe/ZnSe core/shell nanocrystals is the diffusion of Zn^{2+} ions by dissociation of bonds between Zn^{2+} and Se^{2-} ions. The slightly higher activation energy values would arise from the activation energy required for the diffusion of Zn^{2+} ions in CdSe matrices since total activation energy for diffusion-controlled reactions is the summation of the dissociation energy of ions and the energy for diffusion through the matrices. Thus, using the Arrhenius analysis results, the Jander equation for the solid-solution formation was completed as follows:

$$[1-(1-x)^{1/3}]^2 = (2.522 \times 10^9) \times \exp\left(-\frac{151920}{RT}\right)t \quad (3)$$

One can use this completed Jander equation to estimate the degree of solid-solution formation (x), and thus to design $Cd_{1-x}Zn_xSe$ solid-solution nanocrystals showing a specific wavelength light emission without performing experiments.

In contrast to the previous research results, in this study, partial solid-solution formation was achieved though the controlled heat treatment of CdSe/ZnSe core/shell nanocrystals at a certain temperature within a reasonable time period. In reality, another core/shell-type $Cd_{1-x}Zn_xSe/ZnSe$ nanocrystals were obtained in this study. Due to this incomplete solid-solution formation, the surface passivation of the $Cd_{1-x}Zn_xSe$ core can be achieved by the unreacted ZnSe shell. Our PL results showed that the partially solid-solution-treated $Cd_{1-x}Zn_xSe/ZnSe$ nanocrystals had higher PL emission intensity than almost completely solid-solution-treated $Cd_{1-x}Zn_xSe$ nanocrystals. The energy band gap of ZnSe is larger than that of $Cd_{1-x}Zn_xSe$, thus the quantum well structure is still maintained.

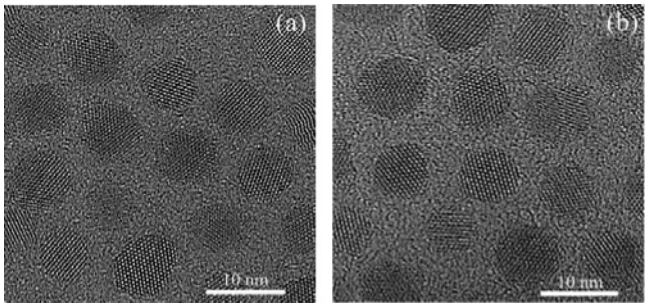

Figure 3. High-resolution transmission electron microscopy (HRTEM) images of (a) as-prepared and (b) heat treated CdSe/ZnSe nanocrystals.

It has been known that Ostwald ripening can be prevented once the solid-solution formation reaction initiates, and thus a narrow size distribution can be maintained during solid-solution heat treatments. HRTEM images in Figure 3a and b show the high crystallinity and the narrow size distribution of CdSe/ZnSe and $Cd_{1-x}Zn_xSe/ZnSe$ nanocrystals, respectively. Furthermore, only slight size increase was detected during heat treatments for the solid-solution formation.

From this study, a kinetics equation for the solid-solution formation was established for CdSe/ZnSe, and the solid-solution formation mechanism was determined as Zn^{2+} ion diffusion in $Cd^{2+}-Se^{2-}$ matrices. This kinetic analysis approach can be applied to the derivation of kinetics equations for other solid-solution formation reactions of II−VI and III−V semiconductor nanocrystals, and it can supply a key not only to estimate but also to control the wavelength of possible light emission from each solid-solution nanocrystal.

Acknowledgment. This study was supported by a Korea University grant of 2005.

Supporting Information Available: The method to determine the degree of solid-solution formation (x) and the kinetics plots are presented. This material is available free of charge via the Internet at http://pubs.acs.org.

References

(1) Murray, C. B.; Norris, D. J.; Bawendi, M. G. *J. Am. Chem. Soc.* **1993**, *115*, 8706.
(2) Alivisatos, A. P. *Science* **1996**, *271*, 933.
(3) Shim, M.; Guyot-Sionnest, P. *Nature* **2000**, *407*, 981.
(4) Qu, L. H.; Yu, W. W.; Peng, X. P. *Nano Lett.* **2004**, *4*, 465.
(5) Bruchez, M. P.; Moronne, M.; Gin, P.; Weiss, S.; Alivisatos, A. P. *Science* **1998**, *281*, 2031.
(6) Peng, X. G.; Schlamp, M. C.; Kadavanich, A. V.; Alivisatos, A. P. *J. Am. Chem. Soc.* **1997**, *119*, 7019.
(7) Dabbousi, B. O.; Rodriguez-Viejo, J.; Mikulec, F. V.; Heine, J. R.; Mattoussi, H.; Ober, R.; Jensen, K. F.; Bawendi, M. G. *J. Phys. Chem. B* **1997**, *101*, 9463.
(8) Reiss, P.; Bleuse, J.; Pron, A. *Nano Lett.* **2002**, *2*, 781.
(9) Zhong, X.; Feng, Y.; Knoll, W.; Han, M. *J. Am. Chem. Soc.* **2003**, *125*, 13559.
(10) Zhong, X.; Han, M.; Dong, Z.; White, T. J.; Knoll, W. *J. Am. Chem. Soc.* **2003**, *125*, 8589.
(11) Zhong, X.; Zhang, Z.; Liu, S.; Han, M.; Knoll, W. *J. Phys. Chem. B* **2004**, *108*, 15552.
(12) Jander, W. *Z. Anorg. U. Allgem. Chem.* **1927**, *163*, 1.

JA061858C